## This file contains:

Supplementary Table 1-5, Supplementary Figure 1-12.

## Supplementary Tables.

**Supplementary Table 1: Demographic data of patients from which *H. pylori*-positive and *H. pylori*-negative gastric samples were harvested.**

| Patient characteristics | *H. pylori*-positive | | *H. pylori*-negative | | *p*-values |
|---|---|---|---|---|---|
| | n | (%, SD) | n | (%, SD) | |
| Demographic characteristics | | | | | |
| Female | 8 | 40% | 11 | 55% | 0.3422 |
| Male | 12 | 60% | 9 | 45% | |
| Age (mean, SD) | 46.7 | 16.15 | 42.6 | 14.93 | 0.4097 |
| Severity of gastritis | | | | | |
| Mild | 2 | 10% | 3 | 10.52% | 0.54 |
| Moderate | 15 | 75% | 16 | 84.21% | |
| Severe | 3 | 15% | 1 | 5.26% | |

Statistical analysis of patient characteristics was performed using Pearson's chi-squared test ('gender' and 'severity of gastritis') and unpaired two-tailed Student's *t*-test ('Age') with *p*-values less than 0.05 considered statistically significant. Source data are provided as a Source Data file.

**Supplementary Table 2: Clinical information of patients from which gastric tissues were harvested before and after antibiotic-based treatment.**

| Patient ID | Average age | Sex | Pathology Description | Sampling Site | Therapy Type |
|---|---|---|---|---|---|
| Patient 1 | 48.8 | M | Gastritis | Antrum | EAC |
| Patient 2 | | F | Gastritis | Antrum | Triple therapy |
| Patient 3 | | F | Gastritis | Antrum | EAC |
| Patient 4 | | M | Gastritis | Antrum | EAC |
| Patient 5 | | F | Gastritis | Antrum | EAC |
| Patient 6 | | F | Gastritis | Antrum | EAC |
| Patient 7 | | M | Gastritis | Antrum | Triple therapy |
| Patient 8 | | F | Gastritis | Antrum | NAC |
| Patient 9 | | M | Gastritis | Antrum | EAC |
| Patient 10 | | F | Gastritis | Antrum | EAC |
| Patient 11 | | F | Gastritis | Antrum | EAC |
| Patient 12 | | F | Gastritis | Antrum | EAC |

M: Male; F: Female; EAC: esomeprazole, amoxicillin and clarithromycin; NAC: N-Acetylcysteine, amoxicillin and clarithromycin; Triple therapy: proton pump inhibitor plus two other types of antibiotics (non-EAC regimen)

**Supplementary Table 3: The inclusion and exclusion criteria of patient recruitment.**

| Inclusion Criteria | Exclusion Criteria |
|---|---|
| 1. Participants aged 18-70 years | 1. Individuals with a history of gastric surgery or other major gastrointestinal disorders (e.g., Crohn's disease, ulcerative colitis) |
| 2. Individuals diagnosed with gastritis by endoscopy | 2. Pregnant or lactating women |
| 3. Consent obtained from participants in the study | 3. Patients with an active bleeding disorder or currently taking anticoagulant medications |
| | 4. Individuals with severe comorbidities (e.g., liver or kidney failure, heart disease) that may affect the study results or patient safety |
| | 5. Participants on antibiotic treatment within the past 2 weeks which may influence *H. pylori* detection |
| | 6. Participants who had received *H. pylori* eradication treatment before |

**Supplementary Table 4: The primers sequences used in this study.**

| Primer name | Sequence (5′ to 3′) |
|---|---|
| *H. pylori*-F | TTTGTTAGAGAAGATAATGACGGTATCTAAC |
| *H. pylori*-R | CATAGGATTTCACACCTGACTGACTATC |
| LOX-1-F | TTGCCTGGGATTAGTAGTGACC |
| LOX-1-R | GCTTGCTCTTGTGTTAGGAGGT |
| LOX-1-MeRIP-F | AGTGCCGACAGCATTGGTG |
| LOX-1-MeRIP-R | GGAGCAGAGGTATCATAGGAAGC |
| ACTB-F | CTTCCCAAGAAGGTTCGATTGA |
| ACTB-R | TCAGACTCTCTTAGGCCAGTTAC |
| GAPDH-F | ACTTGGCTCCCTTATCTGACC |
| GAPDH-R | TGTGCAGTGTGAGAAAGGCTT |
| Il1b-F | GCAACTGTTCCTGAACTCAACT |
| Il1b-R | ATCTTTTGGGGTCCGTCAACT |
| Il6-F | TAGTCCTTCCTACCCCAATTTCC |
| Il6-R | TTGGTCCTTAGCCACTCCTTC |
| Tnf-F | CCCTCACACTCAGATCATCTTCT |
| Tnf-R | GCTACGACGTGGGCTACAG |
| Actb-F | GGCTGTATTCCCCTCCATCG |
| Actb-R | CCAGTTGGTAACAATGCCATGT |
| Up_F | ATGGTTAATAAAGATGTGAAACAAAC |
| Up_R | tagaaaagatcaaaggatcttcCAAAAATCCCATACCATGTCAT |
| Down_F | atgctcgatgagtttttctaaGAGTAATGTTCCTGAAAGCTTATA |
| Down_R | CTTGTAACATCCTATCAGGGCTATAG |
| KanR_F | ATGACATGGTATGGGATTTTTGgaagatcctttgatcttttctac |
| KanR_R | AAGCTTTCAGGAACATTACTCttagaaaaactcatcgagcatcaaa |
| *katA*-BamHI-F | CGGTACCCGGGGATCATGGTTAATAAAGATGTGAAAC |
| *katA*-NheI-R | GCTCGCGAAAGCTAGTTACTTTTTCTTTTTTGTGTGG |
| *babA*-F | CTTTCCGTGGGGCTTTTTGG |

| | |
|---|---|
| *babA*-R | GGTGGGGATTTTCACGCCTA |
| *sabA*-F | TCAACCGTAAGCAACGCTCT |
| *sabA*-R | TGAAACGCCACTGATGACGA |
| 16S rRNA-F | ACGCATAGGTCATGTGCCTC |
| 16S rRNA-R | GTGTCCGTTCACCCTCTCAG |
| FUT2-F | TCCCCTGGCAGAACTACCA |
| FUT2-R | GGTGAAGCGGACGTACTCC |
| FUT3-F | CTGTCCCGCTGTTCAGAGATG |
| FUT3-R | AGGCGTGACTTAGGGTTGGA |

**Supplementary Table 5: The siRNA sequences used in this study.**

| Gene name | Sequence (5′ to 3′) |
|---|---|
| siMETTL3#1-Sense | CAAGUAUGUUCACUAUGAATT |
| siMETTL3#1-Antisense | UUCAUAGUGAACAUACUUGTT |
| siMETTL3#2-Sense | GACUGCUCUUUCCUUAAUATT |
| siMETTL3#2-Antisense | UAUUAAGGAAAGAGCAGUCTT |
| siMETTL14#1-Sense | GCAGCACCUCGAUCAUUUATT |
| siMETTL14#1-Antisense | UAAAUGAUCGAGGUGCUGCTT |
| siMETTL14#2-Sense | GGUGCCGUGUUAAAUAGCATT |
| siMETTL14#2-Antisense | UGCUAUUUAACACGGCACCTT |
| siWTAP#1-Sense | CCCAGCGAUCAACUUGUUUTT |
| siWTAP#1-Antisense | AAACAAGUUGAUCGCUGGGTC |
| siWTAP#2-Sense | GGGCAACACAACCGAAGAUTT |
| siWTAP#2-Antisense | AUCUUCGGUUGUGUUGCCCTT |
| siLOX-1#1-Sense | CCAUUAUGGUGCUGGGCAUTT |
| siLOX-1#1-Antisense | AUGCCCAGCACCAUAAUGGTT |
| siLOX-1#2-Sense | GCAAGACUGGAUCUGGCAUTT |
| siLOX-1#2-Antisense | AUGCCAGAUCCAGUCUUGCTT |
| siFUT2#1-Sense | CCATCTACCTGGCCAATTATT |
| siFUT2#1-Antisense | TAATTGGCCAGGTAGATGGTT |
| siFUT2#2-Sense | CCACTATATTTCACGTTCATT |
| siFUT2#2-Antisense | TGAACGTGAAATATAGTGGTT |
| siFUT3#1-Sense | GACAGATACTTCAATCTCATT |
| siFUT3#1-Antisense | TGAGATTGAAGTATCTGTCTT |
| siFUT3#2-Sense | ACTGGGATATCATGTCCAATT |
| siFUT3#2-Antisense | TTGGACATGATATCCCAGTTT |

## Supplementary Figures.

### Supplementary Figure 1: m$^6$A levels in gastric tissues harvested from patients before and after antibiotic treatment.

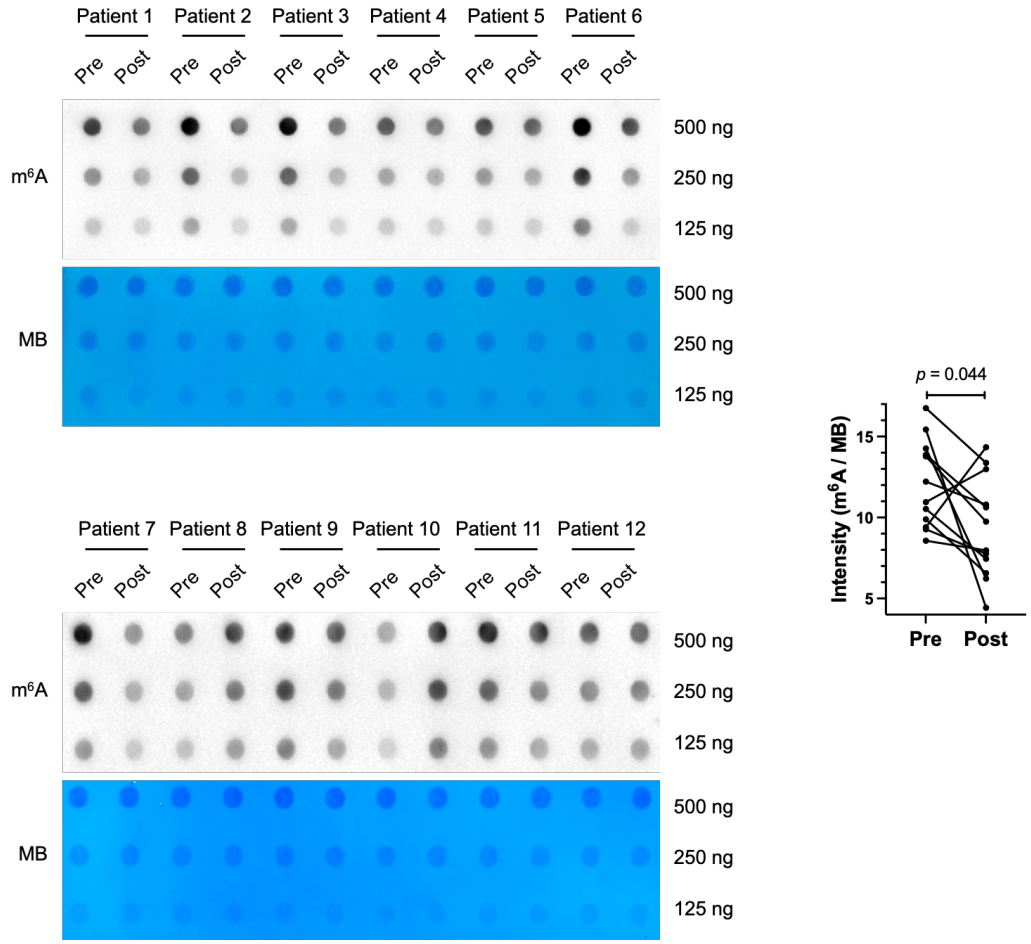


The m$^6$A level of poly(A)$^+$ RNAs in patients' gastric antrum sections (n = 12) before and after treatment with antibiotics was evaluated by m$^6$A dot blot assay. The RNA of each sample was loaded equally with a 2-fold serial dilution. Methylene blue (MB) staining was used as a loading control. The intensity of dots was measured by ImageJ and quantitative analysis was shown as m$^6$A/MB. Quantitative analysis was shown as mean ± SD. Statistical analysis of the data was performed using paired two-tailed Student's *t*-test and the corresponding *p*-values are included in the figure panels. Source data are provided as a Source Data file.

**Supplementary Figure 2: m$^6$A levels in mice with or without *H. pylori* infection.**

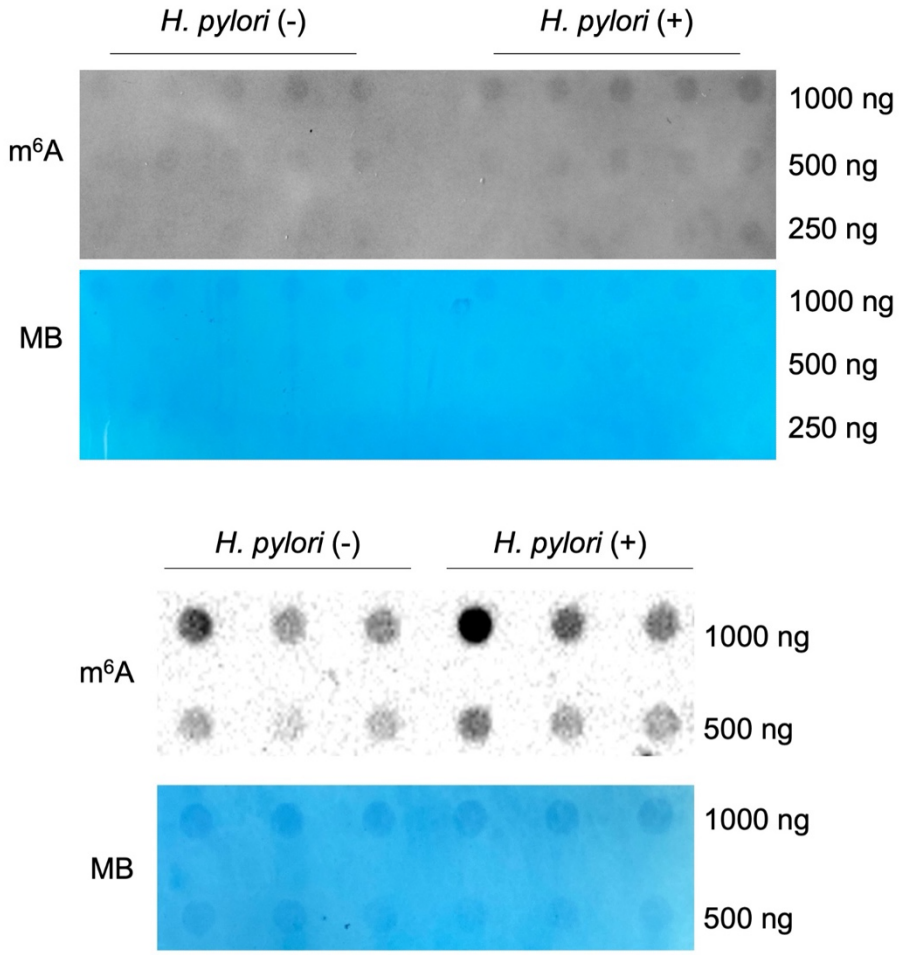


In addition to the 5 samples per group shown in **Fig. 1C**, 8 additional samples per group were shown here. The m$^6$A level of poly(A)$^+$ RNAs in mouse stomach specimens with (n = 13 in total) or without (n = 13 in total) *H. pylori* colonization was evaluated by m$^6$A dot blot assay. The RNA of each sample was loaded equally with a 2-fold serial dilution. Methylene blue (MB) staining was used as a loading control. Source data are provided as a Source Data file.

**Supplementary Figure 3: Volcano plot of differentially methylated RNA sites (DMRS) of m$^6$A-seq**.

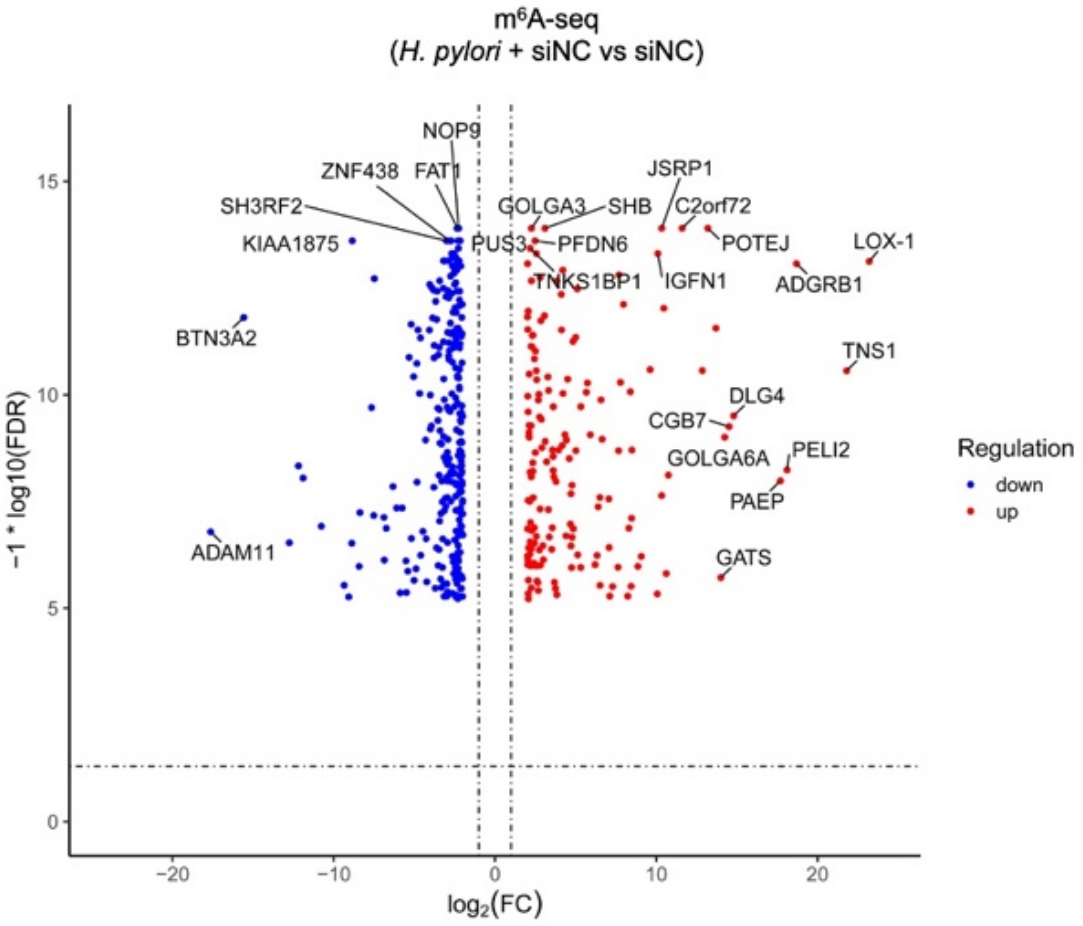


Volcano plot shows the $\log_2$(FC) and -$\log_{10}$(FDR) for all the DMRS (The cut-off of $\log_2$(FC) is larger than 2 and the cut-off of *p*-value is less than 0.0000001). The red dots represent the significantly upregulated genes and the blue dots represent the significantly downregulated genes in the "*H. pylori* + siNC" versus "siNC" comparision. The symbol-marked dots indicate the genes with the most significant FC or FDR. The m$^6$A-seq FC was normalized to the corresponding transcript expression levels in input. FC: fold change; FDR: adjusted *p*-value. Source data are provided as a Source Data file.

**Supplementary Figure 4: Volcano plot of differentially expressed genes (DEG) of RNA-seq**.

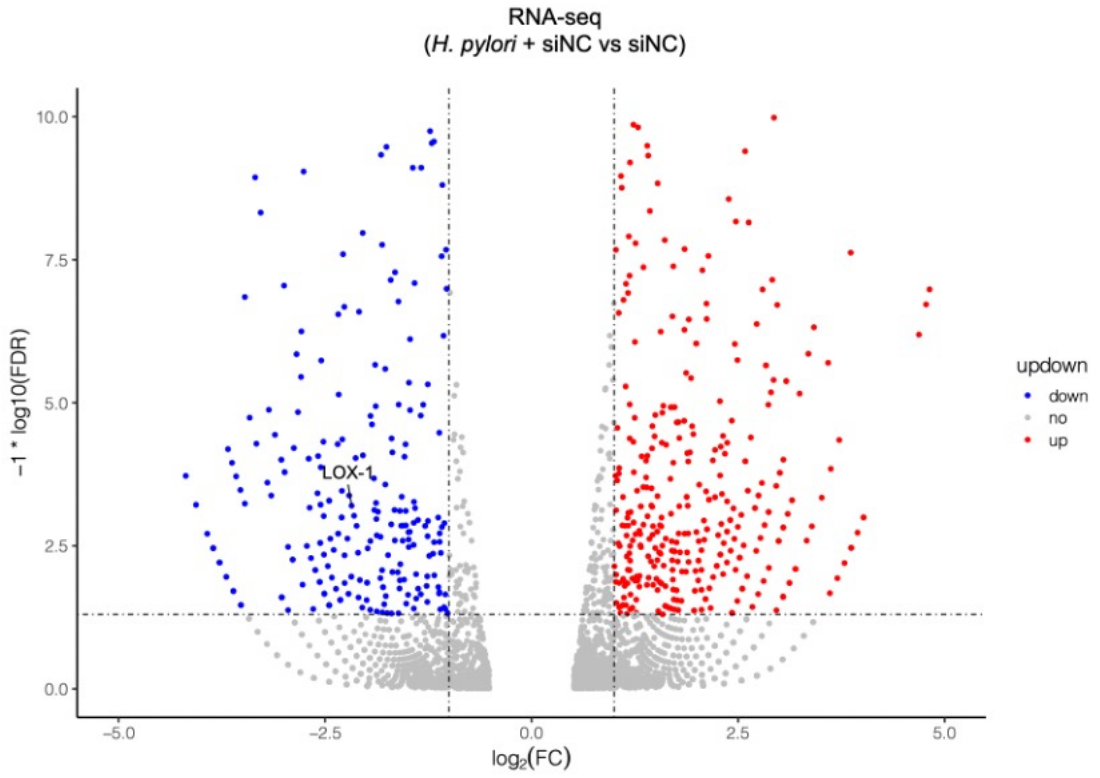


Volcano plot shows the $\log_2$(FC) and -$\log_{10}$(FDR) for all the genes (The cut-off of $\log_2$(FC) is larger than 1 and the cut-off of *p*-value is less than 0.05). The red dots represent the significantly upregulated genes and the blue dots represent the significantly downregulated genes in the "*H. pylori* + siNC" versus "siNC" comparison. FC: fold change; FDR: adjusted *p*-value. Source data are provided as a Source Data file.

**Supplementary Figure 5: Histopathological assessment of *Lox-1* WT and *Lox-1*$^{-/-}$ mice gastric sections.**

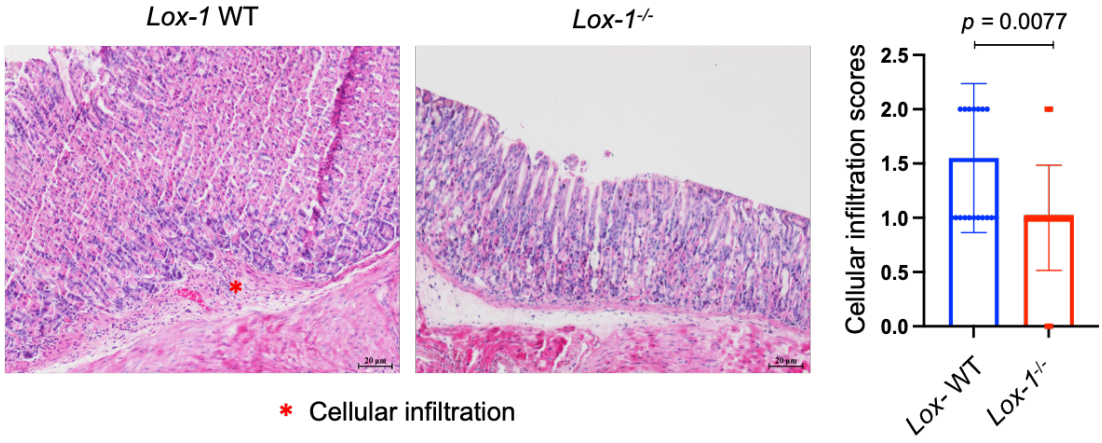


Parafilm-embedded sections of *Lox-1* Wild-type (WT, n = 20 animals) and *Lox-1*$^{-/-}$ mice (n = 18 animals) were stained with hematoxylin and eosin (H&E). Histopathological assessment (cellular infiltration: 0 - 3) was conducted in two separate tissue sections for each animal. Quantitative analysis is shown as mean ± SD. Scale bar, 20 µm. Statistical analysis of the data was performed using unpaired two-tailed Student's *t*-test and the corresponding *p*-values are included in the figure panels. Source data are provided as a Source Data file.

**Supplementary Figure 6: The coating of catalase onto fluorescent beads.**

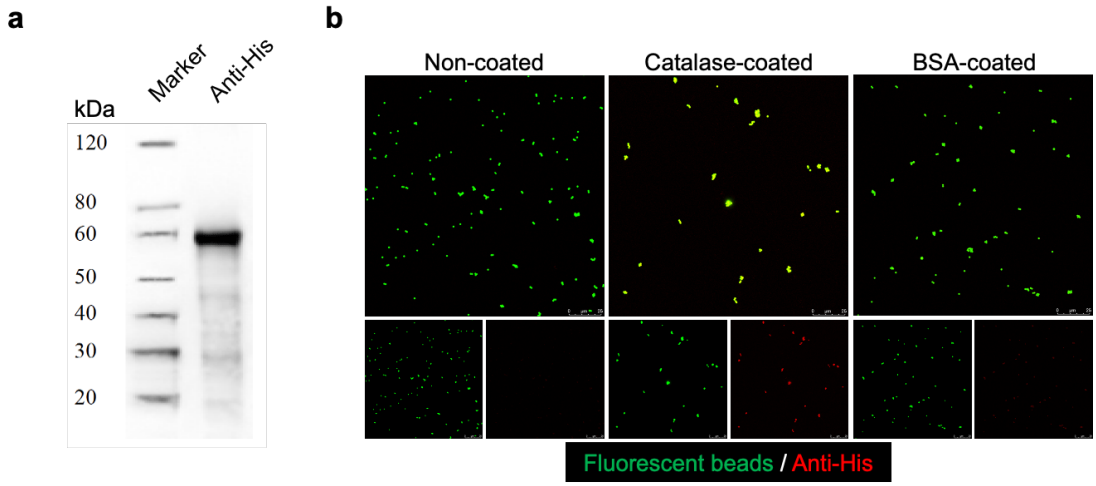


**(a)** Anti-His antibody was used to examine purified recombinant His-tagged catalase proteins of *H. pylori*; **(b)** The coating of recombinant catalase proteins on fluorescent latex beads was confirmed by immunofluorescence assay with anti-His antibody. Source data are provided as a Source Data file.

**Supplementary Figure 7: The construction of isogenic catalase-negative mutant strains.**

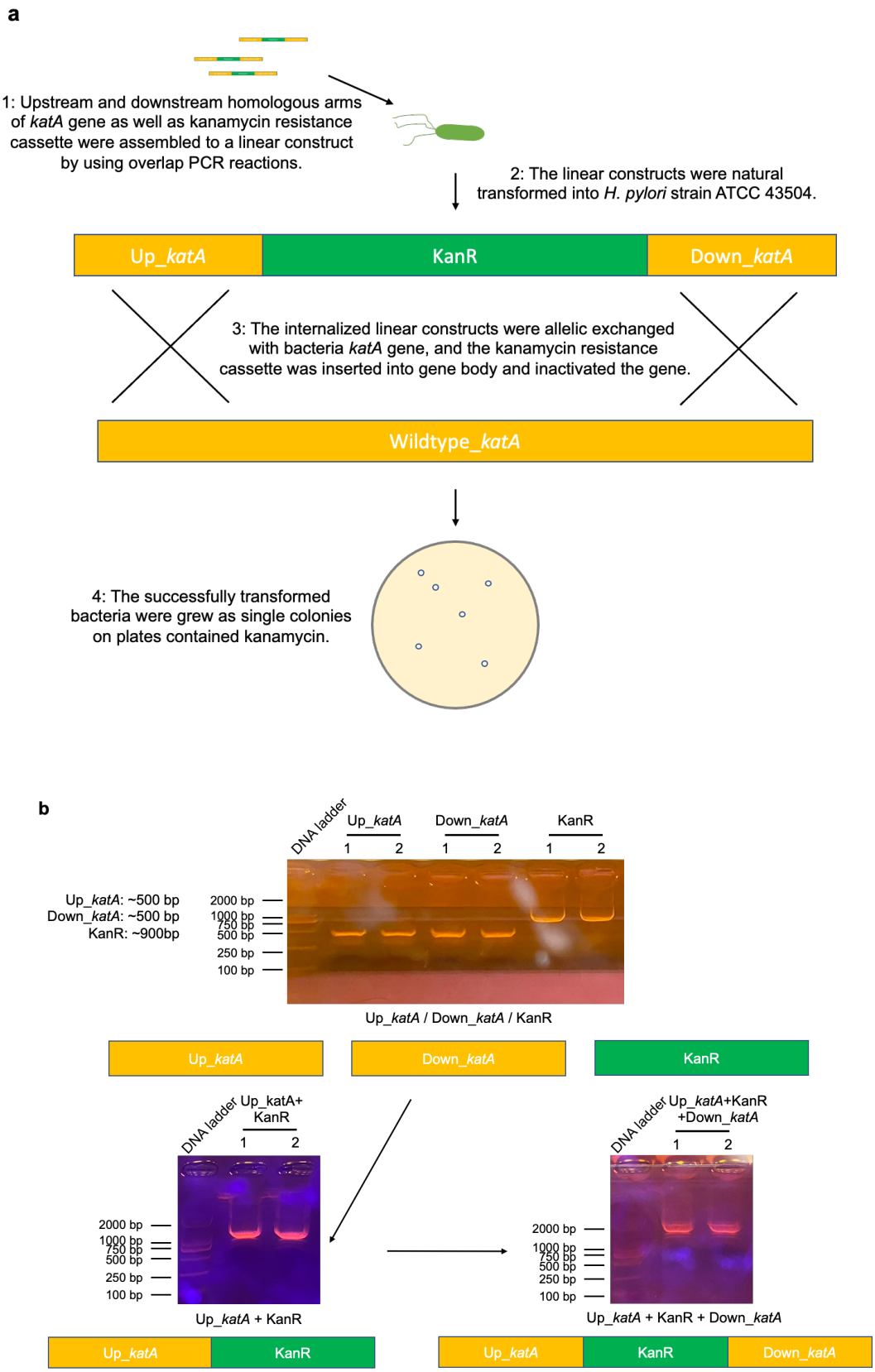

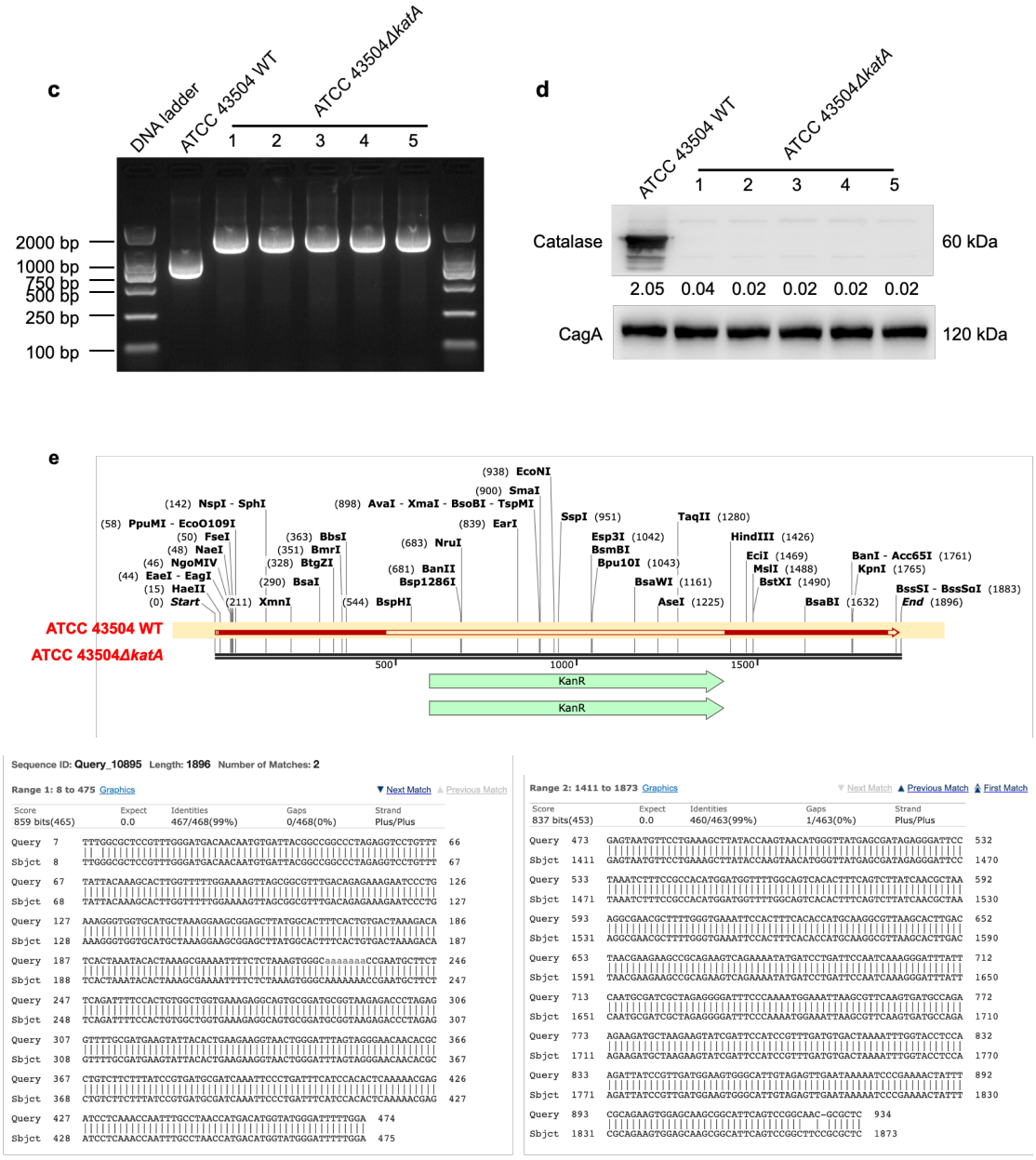


**(a)** Workflow for the allelic exchange method. **(b)** Three fragments, namely Up_*katA*, Down_*katA* and KanR, were PCR-amplified followed by purifiфcation from agarose gel. Two sequential overlap PCR reactions were conducted to assemble three PCR products as a linear construct. **(c, d)** Five single colonies on plates containing 50 μg/mL kanamycin were selected to validate the efficiency of allelic exchange. Agarose gel electrophoresis showed that the PCR products of *katA* gene of five colonies were larger than that of the wild type, indicating that *katA* gene was successfully replaced by the linear construct. The results of Western blots showed that no signal of catalase

could be detected in the five colonies, confirming that the selected colonies were catalase-negative mutants. *H. pylori* CagA was used as an internal control. **(e)** The aligment of sequencing data confirmed that *katA* gene was allelic-exchanged by the linear construct containing the kanamycin resistant cassette (KanR) in the selected colonies. Source data are provided as a Source Data file.

**Supplementary Figure 8: The genetic complementation of *katA*.**

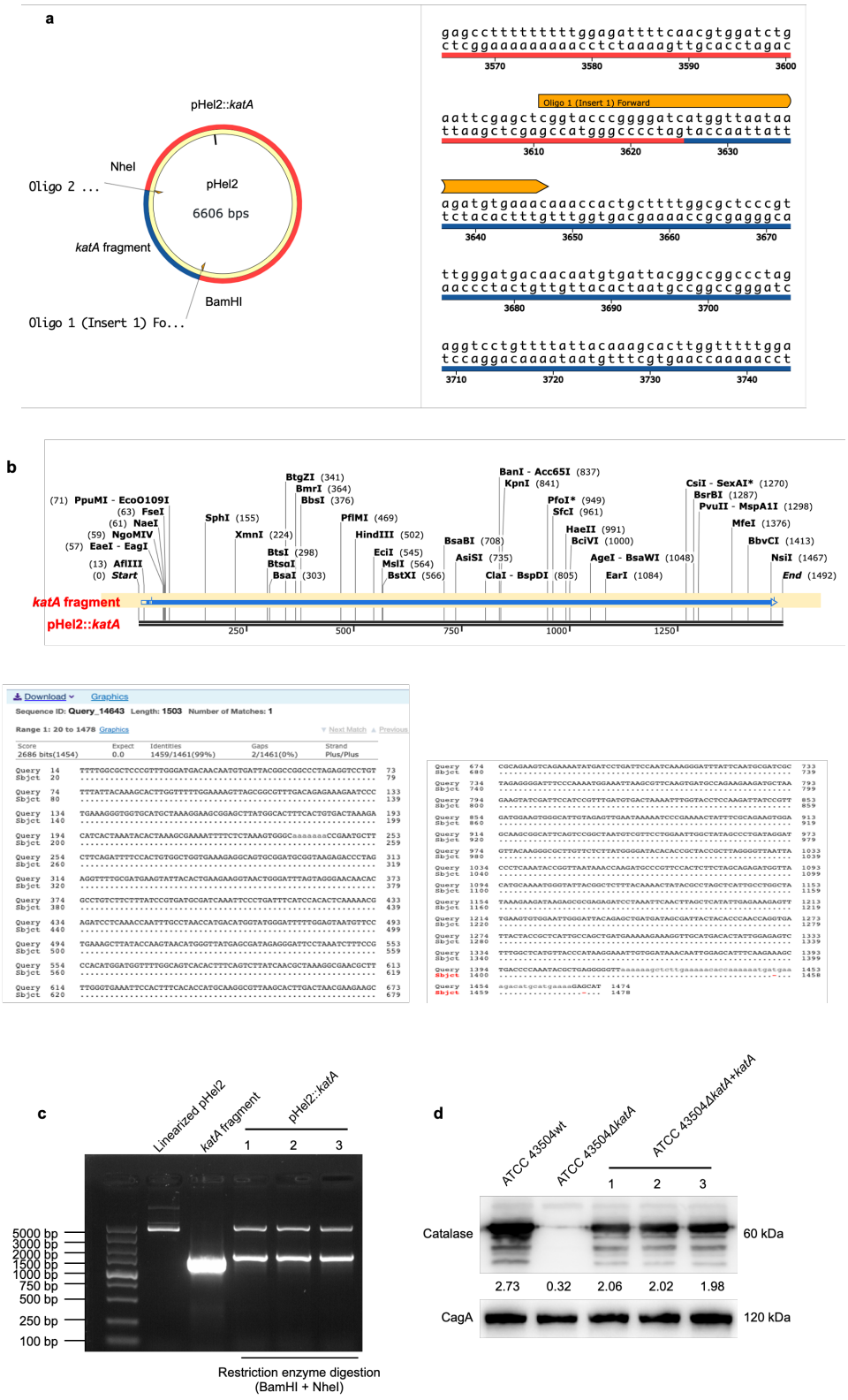


**(a)** The design for construction of pHel2::*katA* using Takara In-Fusion primer design tool (https://takara.teselagen.com/#/DesignPage). **(b)** The sequencing data of

pHel2::*katA* was aligned to the query sequence of *katA* fragment. **(c)** The recombinant vector pHel2::*katA* was digested with two restriction enzymes, BamHI and NheI, followed by agarose gel electrophoresis to confirm the insertion of *katA* fragment. Linearized pHel2 and purified *katA* fragment were used as control. **(d)** The recombinant vector pHel2::*katA* was electroporated into *ΔkatA* mutant. Western blots for detecting catalase was performed to validate the efficiency of genetic complementation of *katA* in mutant strain. *H. pylori* CagA was used as an internal control. Source data are provided as a Source Data file.

**Supplementary Figure 9: Knockout of catalase only affected catalase but not other outer membrane proteins of *H. pylori*.**

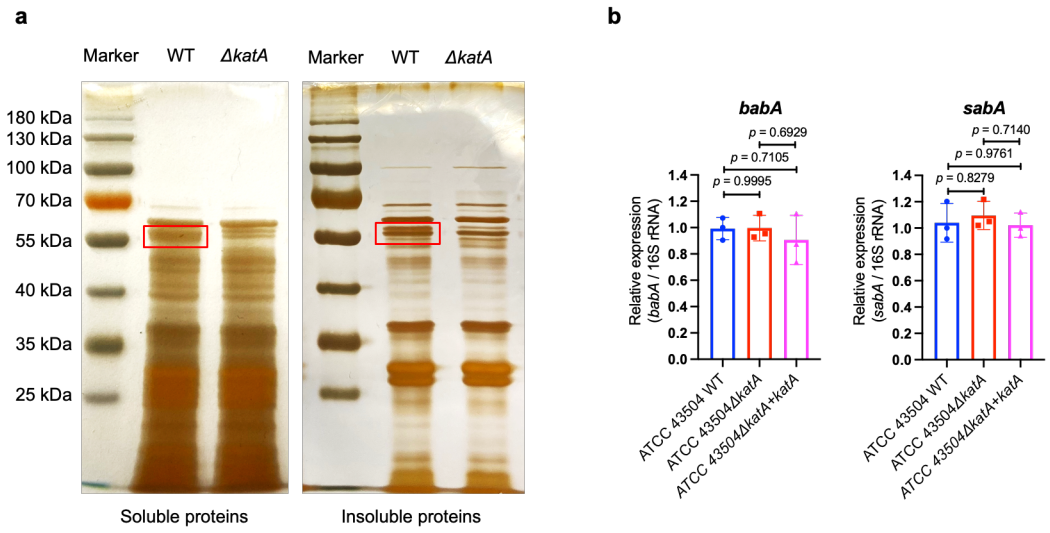


**(a)** Overall soluble and insoluble bacterial proteins were extracted from ATCC 43504 wild-type and *ΔkatA* strains, and analyzed with silver staining. Molecelar size of catalase is 58 kDa. **(b)** qRT-PCR was performed to detect the expression of *babA* and *sabA* in ATCC 43504 wild-type, *ΔkatA* and *ΔkatA+katA* strains. *H. pylori* 16S rRNA was used as an internal control (n = 3 clones for each group). Quantitative data are shown as means ± SD. Statistical analysis of the data was performed using one-way ANOVA followed by Tukey's multiple comparison tests with adjustments and the corresponding *p*-values are included in the figure panels. The statistical significance of the data was calculated from one of three independent experiments with similar results. Source data are provided as a Source Data file.

**Supplementary Figure 10: *H. pylori* strains were labelled with FITC.**

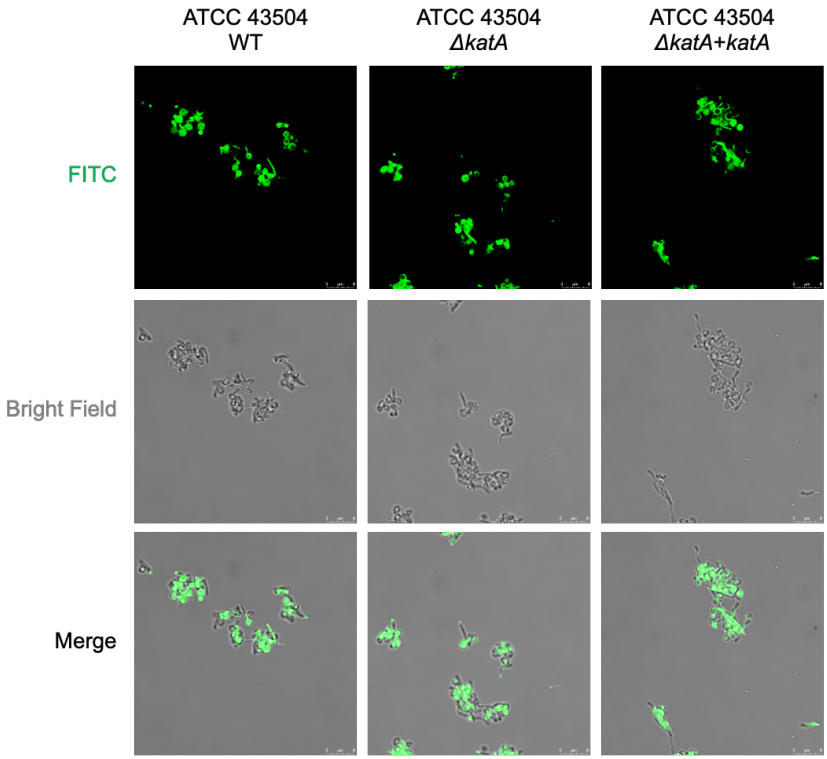


ATCC 43504 wild type, *ΔkatA* and *ΔkatA+katA* strains were labelled by FITC. No obvious difference in morphology or labelling efficiency was observed among the three strains.

**Supplementary Figure 11: Pre-heating human normal stomach tissue array at 60°C did not change the trend of adhesion level of ATCC 43504 wild-type, *ΔkatA* and *ΔkatA+katA* strains.**

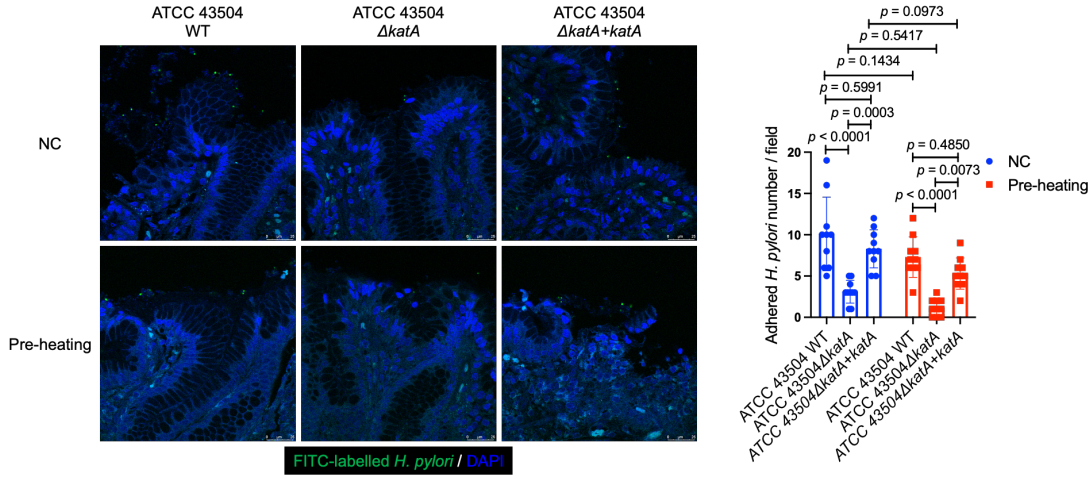


FITC-labelled *H. pylori* strains (wild-type, *ΔkatA* and *ΔkatA+katA* strains) were respectively incubated with human gastric sections with or without pre-heating at 60°C. Ten visual fields of each group were randomly selected to count the number of adhered *H. pylori*. Scale bar, 25 μm. Quantitative data are shown as means ± SD. Statistical analysis of the data was performed using one-way ANOVA followed by Tukey's multiple comparison tests with adjustments and the corresponding *p*-values are included in the figure panels. Source data are provided as a Source Data file.

**Supplementary Figure 12: Detection of *babA* expression in *H. pylori* strains and Lewis$^b$ expression in HFE145 cells.**

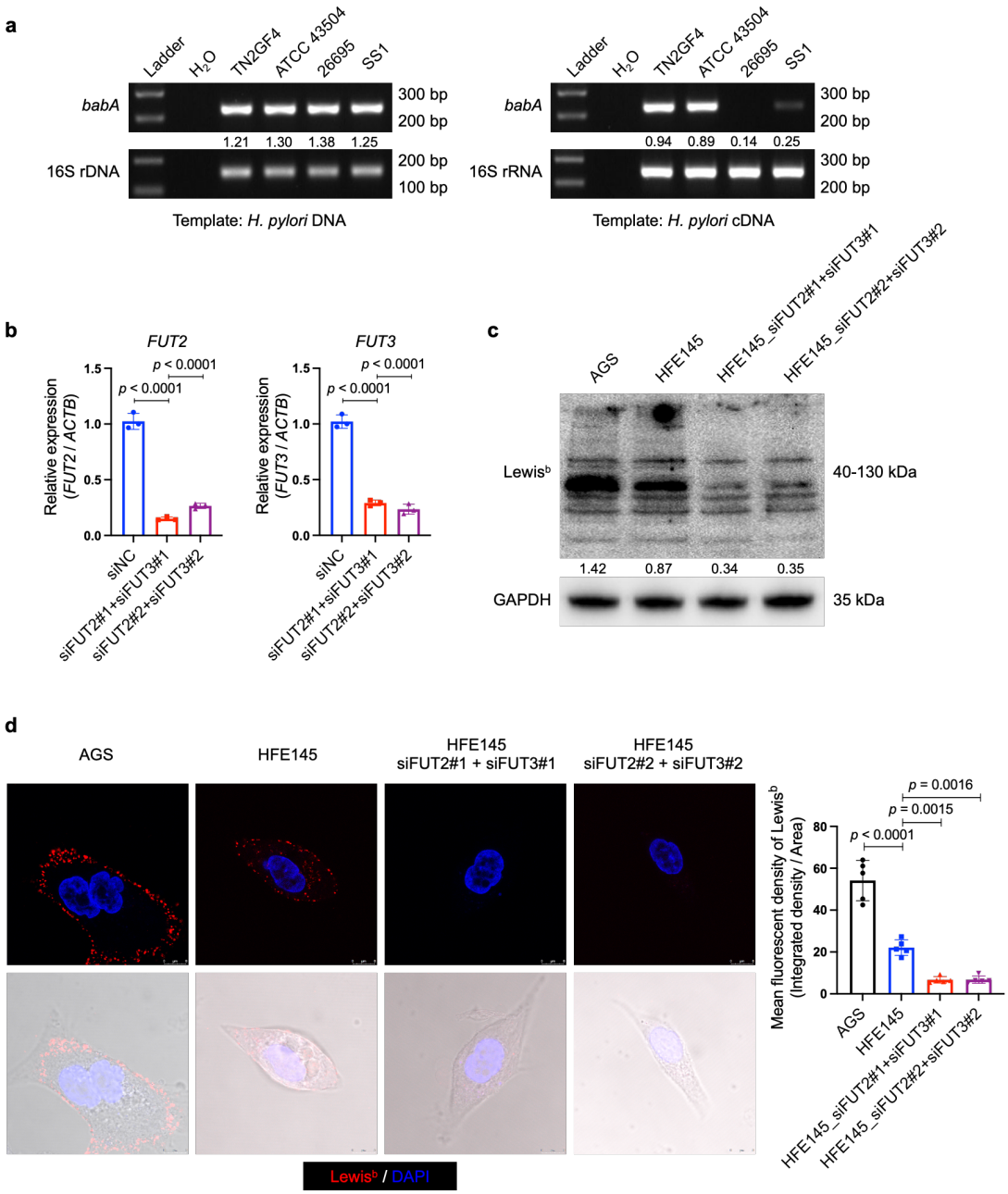


**(a)** Semi-quantitative PCR was performed to detect the expression of *babA* in various *H. pylori* strains. Left panel: *H. pylori* DNA was used as template to test the existence of *babA* gene in different strains. Right panel: *H. pylori* complementary DNA (cDNA) was used as template to measure the levels of *babA* transcript in different strains. **(b)** Two individual siRNAs were transfected into HFE145 cells to knock down *FUT2* and

*FUT3*. The knockdown efficiency was examined by quantitative real-time PCR. *ACTB* was used as an internal control (n = 3 cells for each group). **(c)** Lewis$^b$ expression levels of each group were examined by Western blots. Human GAPDH was used as a loading control. The blots shown are representative of three independent experiments with similar results. **(d)** AGS and HFE145 cells were stained to visualize Lewis$^b$ (red) and the nuclei (Blue). Five visual fields of each group were randomly selected to measure mean fluorescent density of Lewis$^b$. Scale bar, 8 μm. Quantitative data are shown as means ± SD. Statistical analysis of the data was performed using one-way ANOVA followed by Tukey's multiple comparison tests with adjustments and the corresponding *p*-values are included in the figure panels. The statistical significance of the data was calculated from one of three independent experiments with similar results. Source data are provided as a Source Data file.